

Structured Low-Rank Matrix Factorization with Missing and Grossly Corrupted Observations

Fanhua Shang^a, Yuanyuan Liu^b, Hanghang Tong^c, James Cheng^a, Hong Cheng^b

^aDepartment of Computer Science and Engineering, The Chinese University of Hong Kong

^bDepartment of Systems Engineering and Engineering Management, The Chinese University of Hong Kong

^cSchool of computing informatics and decision systems engineering, Arizona State University

Abstract

Recovering low-rank and sparse matrices from incomplete or corrupted observations is an important problem in machine learning, statistics, bioinformatics, computer vision, as well as signal and image processing. In theory, this problem can be solved by the natural convex joint/mixed relaxations (i.e., l_1 -norm and trace norm) under certain conditions. However, all current provable algorithms suffer from superlinear per-iteration cost, which severely limits their applicability to large-scale problems. In this paper, we propose a scalable, provable structured low-rank matrix factorization method to recover low-rank and sparse matrices from missing and grossly corrupted data, i.e., robust matrix completion (RMC) problems, or incomplete and grossly corrupted measurements, i.e., compressive principal component pursuit (CPCP) problems. Specifically, we first present two small-scale matrix trace norm regularized bilinear structured factorization models for RMC and CPCP problems, in which repetitively calculating SVD of a large-scale matrix is replaced by updating two much smaller factor matrices. Then, we apply the alternating direction method of multipliers (ADMM) to efficiently solve the RMC problems. Finally, we provide the convergence analysis of our algorithm, and extend it to address general CPCP problems. Experimental results verified both the efficiency and effectiveness of our method compared with the state-of-the-art methods.

Keywords: Compressive principal component pursuit, Robust matrix completion, Robust principal component analysis, Low-rank matrix recovery and completion

1. Introduction

In recent years, recovering low-rank and sparse matrices from severely incomplete or even corrupted observations has received broad attention in many different fields, such as statistics [1, 2, 3], bioinformatics [4], machine learning [5, 6, 7, 8], computer vision [9, 10, 11, 12, 13], signal and image processing [14, 15, 16, 17, 18]. In those areas, the data to be analyzed often have high dimensionality, which brings great challenges to data analysis, such as digital photographs, surveillance videos, text and web documents. Fortunately, the high-dimensional data are observed to have low intrinsic dimension, which is often much smaller than the dimension of the ambient space [19].

*Corresponding author, e-mail: fhshang@cse.cuhk.edu.hk

For the high-dimensional data, principal component analysis (PCA) is one of the most popular analysis tools to recover a low-rank structure of the data mainly because it is simple to implement, can be solved efficiently, and is effective in many real-world applications such as face recognition and text clustering. However, one of the main challenges faced by PCA is that the observed data is often contaminated by outliers and missing values [20], or is a small set of linear measurements [1]. To address these issues, many compressive sensing or rank minimization based techniques and methods have been proposed, such as robust PCA [5, 21, 13] (RPCA, also called PCP in [9] and low-rank and sparse matrix decomposition in [7, 22], LRSD) and low-rank matrix completion [23, 3].

In many applications, we have to recover a matrix from only a small number of observed entries, for example collaborative filtering for recommender systems. This problem is often called matrix completion, where missing entries or outliers are presented at arbitrary location in the measurement matrix. Matrix completion has been used in a wide range of problems such as collaborative filtering [23, 3], structure-from-motion [24, 11], click prediction [25], tag recommendation [26], and face reconstruction [27]. In some other applications, we would like to recover low-rank and sparse matrices from corrupted data. For example, the face images of a person may be corrupted by glasses or shadows [28]. The classical PCA cannot address the issue as its least-squares fitting is sensitive to these gross outliers. Recovering a low-rank matrix in the presence of outliers has been extensively studied, which is often called RPCA, PCP or LRSD. The RPCA problem has been successfully applied in many important applications, such as latent semantic indexing [29], video surveillance [5, 9], and image alignment [15]. In some more general applications, we also have to simultaneously recover both low-rank and sparse matrices from small sets of linear measurements, which is called compressive principal component pursuit (CPCP) in [1].

In principle, those problems mentioned above can be exactly solved with high probability under mild assumptions via a hybrid convex program involving both the l_1 -norm and the trace norm (also called the nuclear norm) minimization. In recent years, many new techniques and algorithms [23, 3, 9, 5, 21, 1] for low-rank matrix recovery and completion have been proposed, and the theoretical guarantees have been derived in [23, 9, 1]. However, those provable algorithms all exploit a closed-form expression for the proximal operator of the trace norm, which involves the singular value decomposition (SVD). Hence, they all have high computational cost and are even not applicable for solving large-scale problems.

To address this issue, we propose a scalable robust bilinear structured factorization (RBF) method to recover low-rank and sparse matrices from incomplete, corrupted data or a small set of linear measurements, which is formulated as follows:

$$\min_{L, S} f(L, S) + \lambda \|L\|_*, \quad \text{s.t.}, \mathcal{A}(L + S) = y, \quad (1)$$

where $\lambda \geq 0$ is a regularization parameter, $\|L\|_*$ is the trace norm of a low-rank matrix $L \in \mathbb{R}^{m \times n}$, i.e., the sum of its singular values, $S \in \mathbb{R}^{m \times n}$ is a sparse error matrix, $y \in \mathbb{R}^p$ is the given linear measurements, $\mathcal{A}(\cdot)$ is an underdetermined linear operator such as the linear projection operator \mathcal{P}_Ω , and $f(\cdot)$ denotes the loss function such as the l_2 -norm loss or the l_1 -norm loss functions.

Unlike existing robust low-rank matrix factorization approaches, our method not only takes into account the fact that the observation is contaminated by additive outliers (Fig. 1 shows an example) or missing data, i.e., robust matrix completion [3, 30] (RMC, also called RPCA plus matrix completion) problems, but can also identify both low-rank and sparse noisy components from incomplete and grossly corrupted measurements, i.e., CPCP problems. We also present a

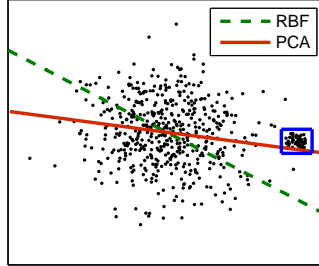


Figure 1: Principal directions learned by PCA and RBF on the toy data set with outliers, which are in a blue rectangle.

robust bilateral factorization framework for both RMC and CPCP problems, in which repetitively calculating SVD of a large matrix in [23, 9, 1] is replaced by updating two much smaller factor matrices. We verify with convincing experimental results both the efficiency and effectiveness of our RBF method.

The main contributions of this paper are summarized as follows:

1. We propose a scalable structured RBF framework to simultaneously recover both low-rank and sparse matrices for both RMC and CPCP problems. By imposing the orthogonality constraint, we convert the original RMC and CPCP models into two smaller-scale matrix trace norm regularized problems, respectively.
2. By the fact that the optimal solution $S_{\Omega^c} = 0$, i.e., the values of S at unobserved locations are zero, we reformulate the proposed RMC problem by replacing the linear projection operator constraint with a simple equality one.
3. Moreover, we propose an efficient alternating direction method of multipliers (ADMM) to solve our RMC problems, and then extend it to address CPCP problems with a linearization technique.
4. Finally, we theoretically analyze the suboptimality of the solution produced by our algorithm.

The remainder of this paper is organized as follows. We review background and related work in Section 2. In Section 3, we propose two scalable trace norm regularized RBF models for RMC and CPCP problems. We develop an efficient ADMM algorithm for solving RMC problems and then extend it to solve CPCP problems in Section 4. We provide the theoretical analysis of our algorithm in Section 5. We report empirical results in Section 6, and conclude this paper in Section 7.

2. BACKGROUND

A low-rank structured matrix $L \in \mathbb{R}^{m \times n}$ and a sparse one $S \in \mathbb{R}^{m \times n}$ can be recovered from highly corrupted measurements $y = \mathcal{P}_Q(D) \in \mathbb{R}^p$ via the following CPCP model,

$$\min_{L, S} \|S\|_1 + \lambda \|L\|_*, \quad \text{s.t.}, \mathcal{P}_Q(D = L_0 + S_0) = \mathcal{P}_Q(L + S), \quad (2)$$

where $\|S\|_1$ denotes the l_1 -norm of S , i.e., $\|S\|_1 = \sum_{ij} |s_{ij}|$, $Q \subseteq \mathbb{R}^{m \times n}$ is a linear subspace, and \mathcal{P}_Q is the projection operator onto that subspace. When $\mathcal{P}_Q = \mathcal{P}_\Omega$, the model (2) is the robust

matrix completion (RMC) problem, where Ω is the index set of observed entries. Wright et al., [1] proved the following result.

Theorem 1. *Let $L_0, S_0 \in \mathbb{R}^{m \times n}$, with $m \geq n$, and suppose that $L_0 \neq \mathbf{0}$ is a μ -incoherent matrix of rank r ,*

$$r \leq \frac{c_1 n}{\mu \log^2 m},$$

and $\text{sign}(S_0)$ is i.i.d. Bernoulli–Rademacher with non-zero probability $\rho < c_2$. Let $Q \subset \mathbb{R}^{m \times n}$ be a random subspace of dimension

$$\dim(Q) \geq C_1(\rho mn + mr) \log^2 m,$$

distributed according to the Haar measure, probabilistically independent of $\text{sign}(S_0)$. Then the minimizer to the problem (2) with $\lambda = \sqrt{m}$ is unique and equal to (L_0, S_0) with probability at least $1 - C_2 m^{-9}$, where c_1, c_2, C_1 and C_2 are positive numerical constants.

This theorem states that a commensurately small number of measurements are sufficient to accurately recover the low-rank and sparse matrices with high probability. Indeed, if Q is the entire space, the model (2) degenerates to the following RPCA problem [5, 9]

$$\min_{L, S} \|S\|_1 + \lambda \|L\|_*, \quad \text{s.t.}, D = L + S, \quad (3)$$

where D denotes the given observations. Several algorithms have been developed to solve the convex optimization problem (3), such as IALM [31] and LRSD [22]. Although both models (2) and (3) are convex optimization problems, and their algorithms converge to the globally optimal solution, they involve SVD at each iteration and suffer from a high computational cost of $O(mn^2)$. While there have been many efforts towards fast SVD computation such as partial SVD [31] and approximate SVD [32], the performance of these existing methods is still unsatisfactory for many real applications. To address this problem, we propose a scalable, provable robust bilinear factorization method with missing and grossly corrupted observations.

3. OUR RBF FRAMEWORK

Matrix factorization is one of the most useful tools in scientific computing and high dimensional data analysis, such as the QR decomposition, the LU decomposition, SVD, and NMF. In this paper, robust bilinear factorization (RBF) aims to find two smaller low-rank matrices $U \in \mathbb{R}^{m \times d}$ ($U^T U = I$) and $V \in \mathbb{R}^{n \times d}$ whose product is equal to the desired matrix of low-rank, $L \in \mathbb{R}^{m \times n}$,

$$L = UV^T,$$

where d is an upper bound for the rank of L , i.e., $d \geq r = \text{rank}(L)$.

3.1. RMC Model

Suppose that the observed matrix D is corrupted by outliers and missing data, the RMC problem is given by

$$\min_{L, S} \|S\|_1 + \lambda \|L\|_*, \quad \text{s.t.}, \mathcal{P}_\Omega(D) = \mathcal{P}_\Omega(L + S). \quad (4)$$

From the optimization problem (4), we easily find the optimal solution $S_{\Omega^c} = 0$, where Ω^c is the complement of Ω , i.e., the index set of unobserved entries. Consequently, we have the following lemma.

Lemma 2. *The RMC model (4) with the operator \mathcal{P}_Ω is equivalent to the following problem*

$$\min_{L, S} \|\mathcal{P}_\Omega(S)\|_1 + \lambda \|L\|_*, \quad \text{s.t., } \mathcal{P}_\Omega(D) = \mathcal{P}_\Omega(L + S) \text{ and } \mathcal{P}_{\Omega^c}(S) = \mathbf{0}. \quad (5)$$

The proof of this lemma can be found in APPENDIX A. From the incomplete and corrupted matrix D , our RBF model is to find two smaller matrices, whose product approximates L , can be formulated as follows:

$$\begin{aligned} \min_{U, V, S} \quad & \|\mathcal{P}_\Omega(S)\|_1 + \lambda \|UV^T\|_*, \\ \text{s.t., } \quad & \mathcal{P}_\Omega(D) = \mathcal{P}_\Omega(UV^T + S). \end{aligned} \quad (6)$$

Lemma 3. *Let U and V be two matrices of compatible dimensions, where U has orthogonal columns, i.e., $U^T U = I$, then we have $\|UV^T\|_* = \|V\|_*$.*

The proof of this lemma can be found in APPENDIX B. By imposing $U^T U = I$ and substituting $\|UV^T\|_* = \|V\|_*$ into (6), we arrive at a much smaller-scale matrix trace norm minimization problem

$$\begin{aligned} \min_{U, V, S} \quad & \|\mathcal{P}_\Omega(S)\|_1 + \lambda \|V\|_*, \\ \text{s.t., } \quad & \mathcal{P}_\Omega(D) = \mathcal{P}_\Omega(UV^T + S), \quad U^T U = I. \end{aligned} \quad (7)$$

Theorem 4. *Suppose (L^*, S^*) is a solution of the problem (5) with $\text{rank}(L^*) = r$, then there exists the solution $U_k \in \mathbb{R}^{m \times d}$, $V_k \in \mathbb{R}^{n \times d}$ and $S_k \in \mathbb{R}^{m \times n}$ to the problem (7) with $d \geq r$ and $S_{\Omega^c} = 0$, $(U_k V_k^T, S_k)$ is also a solution to the problem (5).*

The proof of this theorem can be found in APPENDIX C.

3.2. CPCP Model

From a small set of linear measurements $y \in \mathbb{R}^p$, the CPCP problem is to recover low-rank and sparse matrices as follows,

$$\begin{aligned} \min_{U, V, S} \quad & \|S\|_1 + \lambda \|V\|_*, \\ \text{s.t., } \quad & \mathcal{P}_\Omega(D) = \mathcal{P}_\Omega(UV^T + S). \end{aligned} \quad (8)$$

Theorem 5. *Suppose (L^*, S^*) is a solution of the problem (2) with $\text{rank}(L^*) = r$, then there exists the solution $U_k \in \mathbb{R}^{m \times d}$, $V_k \in \mathbb{R}^{n \times d}$ and $S_k \in \mathbb{R}^{m \times n}$ to the problem (8) with $d \geq r$, $(U_k V_k^T, S_k)$ is also a solution to the problem (2).*

We omit the proof of this theorem since it is very similar to that of Theorem 4. In the following, we will discuss how to solve the models (7) and (8). It is worth noting that the RPCA problem can be viewed as a special case of the RMC problem (7) when all entries of the corrupted matrix are directly observed. In the next section, we will mainly develop an efficient alternating direction method of multipliers (ADMM) solver for solving the non-convex problem (7). It is also worth noting that although our algorithm will produce different estimations of U and V , the estimation of UV^T is stable as guaranteed by Theorems 4 and 5, and the convexity of the problems (2) and (4).

3.3. Connections to Existing Approaches

According to the discussion above, it is clear that our RBF method is a scalable method for both RMC and CPCP problems. Compared with convex algorithms such as common RPCA [9] and CPCP [1] methods, which have a computational complexity of $O(mn^2)$ and are impractical for solving relatively large-scale problems, our RBF method has a linear complexity and scales well to handle large-scale problems.

To understand better the superiority of our RBF method, we compare and relate RBF with several popular robust low-rank matrix factorization methods. It is clear that the model in [33, 10, 27] is a special case of our trace norm regularized model (7), while $\lambda = 0$. Moreover, the models used in [11, 12] focus only on the desired low-rank matrix. In this sense, they can be viewed as special cases of our model (7). The other major difference is that SVD is used in [11], while QR factorizations are used in this paper. The use of QR factorizations also makes the update operation highly scalable on modern parallel architectures [34]. Regarding the complexity, it is clear that both schemes have the similar theory computational complexity. However, from the experimental results in Section 6, we can see that our algorithm usually runs much faster, but more accurate than the methods in [11, 12]. The following bilinear spectral regularized matrix factorization formulation in [12] is one of the most similar models to our model (7),

$$\min_{L, U, V} \|W \odot (D - L)\|_1 + \frac{\lambda}{2} (\|U\|_F^2 + \|V\|_F^2), \quad \text{s.t., } L = UV^T,$$

where \odot denotes the Hadamard product and $W \in \mathbb{R}^{m \times n}$ is a weight matrix that can be used to denote missing data (i.e., $w_{ij} = 0$).

4. OPTIMIZATION ALGORITHM

In this section, we propose an efficient alternating direction method of multipliers (ADMM) for solving the RMC problem (7), and then extend it for solving the CPCP problem (8). We provide the convergence analysis of our algorithm in Section 5.

4.1. Formulation

Recently, it has been shown in the literature [35, 36] that ADMM is very efficient for some convex or non-convex programming problems from various applications. We also refer to a recent survey [35] for some recently exploited applications of ADMM. For efficiently solving the RMC problem (7), we can assume without loss of generality that the unknown entries of D are simply set as zeros, i.e., $D_{\Omega^c} = 0$, and S_{Ω^c} may be any values such that $\mathcal{P}_{\Omega^c}(D) = \mathcal{P}_{\Omega^c}(UV^T) + \mathcal{P}_{\Omega^c}(S)$. Therefore, the constraint with the operator \mathcal{P}_{Ω} in (7) is simplified into $D = UV^T + S$. Hence, we introduce the constraint $D = UV^T + S$ into (7), and obtain the following equivalent form:

$$\begin{aligned} \min_{U, V, S} \quad & \|\mathcal{P}_{\Omega}(S)\|_1 + \lambda \|V\|_*, \\ \text{s.t.,} \quad & D = UV^T + S, \quad U^T U = I. \end{aligned} \quad (9)$$

The partial augmented Lagrangian function of (9) is

$$\begin{aligned} \mathcal{L}_{\alpha}(U, V, S, Y) = & \lambda \|V\|_* + \|\mathcal{P}_{\Omega}(S)\|_1 \\ & + \langle Y, D - S - UV^T \rangle + \frac{\alpha}{2} \|D - S - UV^T\|_F^2, \end{aligned} \quad (10)$$

where $Y \in \mathbb{R}^{m \times n}$ is a matrix of Lagrange multipliers, $\alpha > 0$ is a penalty parameter, and $\langle M, N \rangle$ denotes the inner product between matrices M and N of equal sizes, i.e., $\langle M, N \rangle = \sum_{i,j} M_{ij} N_{ij}$.

4.2. Robust Bilateral Factorization Scheme

We will derive our scheme for solving the following subproblems with respect to U , V and S , respectively,

$$\begin{aligned} U_{k+1} &= \arg \min_{U \in \mathbb{R}^{m \times d}} \mathcal{L}_{\alpha_k}(U, V_k, S_k, Y_k), \\ &\text{s.t., } U^T U = I, \end{aligned} \quad (11)$$

$$V_{k+1} = \arg \min_{V \in \mathbb{R}^{n \times d}} \mathcal{L}_{\alpha_k}(U_{k+1}, V, S_k, Y_k), \quad (12)$$

$$S_{k+1} = \arg \min_{S \in \mathbb{R}^{m \times n}} \mathcal{L}_{\alpha_k}(U_{k+1}, V_{k+1}, S, Y_k). \quad (13)$$

4.2.1. Updating U

Fixing V and S at their latest values, and by removing the terms that do not depend on U and adding some proper terms that do not depend on U , the problem (11) with respect to U is reformulated as follows:

$$\min_U \|UV_k^T - P_k\|_F^2, \quad \text{s.t., } U^T U = I, \quad (14)$$

where $P_k = D - S_k + Y_k/\alpha_k$. In fact, the optimal solution can be given by the SVD of the matrix $P_k V_k$ as in [37]. To further speed-up the calculation, we introduce the idea in [36] that uses a QR decomposition instead of SVD. The resulting iteration step is formulated as follows:

$$U_{k+1} = Q, \quad \text{QR}(P_k V_k) = QR, \quad (15)$$

where U_{k+1} is an orthogonal basis for the range space $\mathcal{R}(P_k V_k)$, i.e., $\mathcal{R}(U_{k+1}) = \mathcal{R}(P_k V_k)$. Although U_{k+1} in (15) is not an optimal solution to (14), our iterative scheme and the one in [38] are equivalent to solve (14) and (16), and their equivalent analysis is provided in Section 5. Moreover, the use of QR factorizations also makes our update scheme highly scalable on modern parallel architectures [34].

4.2.2. Updating V

Fixing U and S , the optimization problem (12) with respect to V can be rewritten as:

$$\min_V \frac{\alpha_k}{2} \|U_{k+1} V^T - P_k\|_F^2 + \lambda \|V\|_*. \quad (16)$$

To solve the convex problem (16), we first introduce the following definition [39].

Definition 1. For any given matrix $M \in \mathbb{R}^{n \times d}$ whose rank is r , and $\mu \geq 0$, the singular value thresholding (SVT) operator is defined as follows:

$$\text{SVT}_\mu(M) = \bar{U} \text{diag}(\max\{\sigma - \mu, 0\}) \bar{V}^T,$$

where $\max\{\cdot, \cdot\}$ should be understood element-wise, $\bar{U} \in \mathbb{R}^{n \times r}$, $\bar{V} \in \mathbb{R}^{d \times r}$ and $\sigma = (\sigma_1, \dots, \sigma_r)^T \in \mathbb{R}^{r \times 1}$ are obtained by SVD of M , i.e., $M = \bar{U} \text{diag}(\sigma) \bar{V}^T$.

Theorem 6. The trace norm minimization problem (16) has a closed-form solution given by:

$$V_{k+1} = \text{SVT}_{\lambda/\alpha_k}(P_k^T U_{k+1}). \quad (17)$$

Proof. The first-order optimality condition for (16) is given by

$$0 \in \lambda \partial \|V\|_* + \alpha_k (V U_{k+1}^T - P_k^T) U_{k+1},$$

where $\partial \|\cdot\|_*$ is the set of subgradients of the trace norm. Since $U_{k+1}^T U_{k+1} = I$, the optimality condition for (16) is rewritten as follows:

$$0 \in \lambda \partial \|V\|_* + \alpha_k (V - P_k^T U_{k+1}). \quad (18)$$

(18) is also the optimality condition for the following convex problem,

$$\min_V \frac{\alpha_k}{2} \|V - P_k^T U_{k+1}\|_F^2 + \lambda \|V\|_*. \quad (19)$$

By Theorem 2.1 in [39], then the optimal solution of (19) is given by (17). \square

4.2.3. Updating S

Fixing U and V , we can update S by solving

$$\min_S \|\mathcal{P}_\Omega(S)\|_1 + \frac{\alpha_k}{2} \|S + U_{k+1} V_{k+1}^T - D - Y_k/\alpha_k\|_F^2. \quad (20)$$

For solving the problem (20), we introduce the following soft-thresholding operator \mathcal{S}_τ :

$$\mathcal{S}_\tau(A_{ij}) := \begin{cases} A_{ij} - \tau, & A_{ij} > \tau, \\ A_{ij} + \tau, & A_{ij} < -\tau, \\ 0, & \text{otherwise.} \end{cases}$$

Then the optimal solution S_{k+1} can be obtained by solving the following two subproblems with respect to S_Ω and S_{Ω^c} , respectively. The optimization problem with respect to S_Ω is first formulated as follows:

$$\min_{S_\Omega} \frac{\alpha_k}{2} \|\mathcal{P}_\Omega(S + U_{k+1} V_{k+1}^T - D - Y_k/\alpha_k)\|_F^2 + \|\mathcal{P}_\Omega(S)\|_1. \quad (21)$$

By the operator \mathcal{S}_τ and letting $\tau = 1/\alpha_k$, the closed-form solution to the problem (21) is given by

$$(S_{k+1})_\Omega = \mathcal{S}_\tau((D - U_{k+1} V_{k+1}^T + Y_k/\alpha_k)_\Omega). \quad (22)$$

Moreover, the subproblem with respect to S_{Ω^c} is formulated as follows:

$$\min_{S_{\Omega^c}} \|\mathcal{P}_{\Omega^c}(S + U_{k+1} V_{k+1}^T - D - Y_k/\alpha_k)\|_F^2. \quad (23)$$

We can easily obtain the closed-form solution by zeroing the gradient of the cost function (23) with respect to S_{Ω^c} , i.e.,

$$(S_{k+1})_{\Omega^c} = (D - U_{k+1} V_{k+1}^T + Y_k/\alpha_k)_{\Omega^c}. \quad (24)$$

Summarizing the analysis above, we obtain an ADMM scheme to solve the RMC problem (7), as outlined in **Algorithm 1**. Our algorithm is essentially a Gauss-Seidel-type scheme of ADMM, and the update strategy of the Jacobi version of ADMM is easily implemented, well

Algorithm 1 Solving RMC problem (7) via ADMM.

Input: $\mathcal{P}_\Omega(D)$, λ and ε .

Output: U , V and S , where S_{Ω^c} is set to 0.

Initialize: $U_0 = \text{eye}(m, d)$, $V_0 = \mathbf{0}$, $Y_0 = \mathbf{0}$, $\alpha_0 = \frac{1}{\|\mathcal{P}_\Omega(D)\|_F}$, $\alpha_{max} = 10^{10}$, and $\rho = 1.1$.

- 1: **while** not converged **do**
 - 2: Update U_{k+1} by (15).
 - 3: Update V_{k+1} by (17).
 - 4: Update S_{k+1} by (22) and (24).
 - 5: Update the multiplier Y_{k+1} by $Y_{k+1} = Y_k + \alpha_k(D - U_{k+1}V_{k+1}^T - S_{k+1})$.
 - 6: Update α_{k+1} by $\alpha_{k+1} = \min(\rho\alpha_k, \alpha_{max})$.
 - 7: Check the convergence condition, $\|D - U_{k+1}V_{k+1}^T - S_{k+1}\|_F < \varepsilon$.
 - 8: **end while**
-

suiting for parallel and distributed computing and hence is particularly attractive for solving large-scale problems [40]. In addition, S_{Ω^c} should be set to 0 for the expected output S . This algorithm can also be accelerated by adaptively changing α . An efficient strategy [31] is to let $\alpha = \alpha_0$ (the initialization in Algorithm 1) and increase α_k iteratively by $\alpha_{k+1} = \rho\alpha_k$, where $\rho \in (1.0, 1.1]$ in general and α_0 is a small constant. Furthermore, U_0 is initialized with $\text{eye}(m, d) := \begin{bmatrix} I_{d \times d} \\ \mathbf{0}_{(m-d) \times d} \end{bmatrix}$. Algorithm 1 is easily used to solve the RPCA problem (3), where all entries of the corrupted matrix are directly observed. Moreover, we introduce an adaptive rank adjusting strategy for our algorithm in Section 4.4.

4.3. Extension for CPCP

Algorithm 1 can be extended to solve the CPCP problem (8) with the complex operator \mathcal{P}_Q , as outlined in **Algorithm 2**, which is to optimize the following augmented Lagrange function

$$\begin{aligned} \mathcal{F}_\alpha(U, V, S, Y) = & \lambda\|V\|_* + \|S\|_1 + \langle Y, y - \mathcal{P}_Q(S + UV^T) \rangle \\ & + \frac{\alpha}{2}\|y - \mathcal{P}_Q(S + UV^T)\|_2^2. \end{aligned} \quad (25)$$

We minimize \mathcal{F}_α with respect to (U, V, S) using a recently proposed linearization technique [41], which resolves such problems where \mathcal{P}_Q is not the identity operator. Specifically, for updating U and V , let $T = UV^T$ and $g(T) = \frac{\alpha_k}{2}\|y - \mathcal{P}_Q(S_k + T) + Y_k/\alpha_k\|_2^2$, then $g(T)$ is approximated by

$$g(T) \approx g(T_k) + \langle \nabla g(T_k), T - T_k \rangle + \tau\|T - T_k\|_F^2, \quad (26)$$

where $\nabla g(T_k) = \alpha_k \mathcal{P}_Q^*(\mathcal{P}_Q(T_k + S_k) - y - Y_k/\alpha_k)$, \mathcal{P}_Q^* is the adjoint operator of \mathcal{P}_Q , and τ is chosen as $\tau = 1/\|\mathcal{P}_Q^* \mathcal{P}_Q\|_2$ as in [41], and $\|\cdot\|_2$ the spectral norm of a matrix, i.e., the largest singular value of a matrix.

Similarly, for updating S , let $T_{k+1} = U_{k+1}V_{k+1}^T$ and $h(S) = \frac{\alpha_k}{2}\|y - \mathcal{P}_Q(S + T_{k+1}) + Y_k/\alpha_k\|_2^2$, then $h(S)$ is approximated by

$$h(S) \approx h(S_k) + \langle \nabla h(S_k), S - S_k \rangle + \tau\|S - S_k\|_F^2, \quad (27)$$

where $\nabla h(S_k) = \alpha_k \mathcal{P}_Q^*(\mathcal{P}_Q(S_k + T_{k+1}) - y - Y_k/\alpha_k)$.

Algorithm 2 Solving CPCP problem (8) via ADMM.

Input: $y \in \mathbb{R}^p$, \mathcal{P}_Q , and parameters λ and ε .

Output: U , V and S .

Initialize: $U_0 = \text{eye}(m, d)$, $V_0 = \mathbf{0}$, $Y_0 = \mathbf{0}$, $\alpha_0 = \frac{1}{\|y\|_2}$, $\alpha_{max} = 10^{10}$, and $\rho = 1.1$.

1: **while** not converged **do**

2: Update U_{k+1} by $U_{k+1} = Q$, $\text{QR}((U_k V_k^T - \nabla g(U_k V_k^T)/\tau)V_k) = QR$.

3: Update V_{k+1} by $V_{k+1}^T = \text{SVT}_{\lambda/\alpha_k}(U_{k+1}^T(U_k V_k^T - \nabla g(U_k V_k^T)/\tau))$.

4: Update S_{k+1} by $S_{k+1} = \mathcal{S}_{1/\alpha_k}(S_k - \nabla h(S_k)/\tau)$.

5: Update the multiplier Y_{k+1} by $Y_{k+1} = Y_k + \alpha_k(y - \mathcal{P}_Q(U_{k+1} V_{k+1}^T + S_{k+1}))$.

6: Update the parameter α_{k+1} by $\alpha_{k+1} = \min(\rho\alpha_k, \alpha_{max})$.

7: Check the convergence condition,

$$(\|T_{k+1} - T_k\|_F^2 + \|S_{k+1} - S_k\|_F^2) / (\|T_k\|_F^2 + \|S_k\|_F^2) < \varepsilon.$$

8: **end while**

4.4. Stopping Criteria and Rank Adjusting Strategy

As the stopping criteria for terminating our RBF algorithms, we employ some gap criteria; that is, we stop Algorithm 1 when the current gap is satisfied as a given tolerance ε , i.e., $\|D - U_k V_k^T - S_k\|_F < \varepsilon$, and run Algorithm 2 when $(\|U_k V_k^T - U_{k-1} V_{k-1}^T\|_F^2 + \|S_k - S_{k-1}\|_F^2) / (\|U_{k-1} V_{k-1}^T\|_F^2 + \|S_{k-1}\|_F^2) < \varepsilon$.

In Algorithms 1 and 2, d is one of the most important parameters. If d is too small, it can cause underfitting and a large estimation error; but if d is too large, it can cause overfitting and large deviation to the underlying low-rank matrix L . Fortunately, several works [42, 36] have provided some matrix rank estimation strategies to compute a good value r for the rank of the involved matrices. Thus, we only set a relatively large integer d such that $d \geq r$. In addition, we provide a scheme to dynamically adjust the rank parameter d . Our scheme starts from an overestimated input, i.e., $d = \lfloor 1.2r \rfloor$. Following [42] and [33], we decrease it aggressively once a dramatic change in the estimated rank of the product $U_k V_k^T$ is detected based on the eigenvalue decomposition which usually occurs after a few iterations. Specifically, we calculate the eigenvalues of $(U_k V_k^T)^T U_k V_k^T = V_k U_k^T U_k V_k^T = V_k V_k^T$, which are assumed to be ordered as $\lambda_1 \geq \lambda_2 \geq \dots \geq \lambda_d$. Since the product $V_k V_k^T$ and $V_k^T V_k$ have the same nonzero eigenvalues, it is much more efficient to compute the eigenvalues of the product $V_k^T V_k$. Then we compute the quotient sequence $\bar{\lambda}_i = \lambda_i / \lambda_{i+1}$, $i = 1, \dots, d-1$. Suppose $\hat{r} = \arg \max_{1 \leq i \leq d-1} \bar{\lambda}_i$. If the condition

$$\text{gap} = \frac{(d-1)\bar{\lambda}_{\hat{r}}}{\sum_{i \neq \hat{r}} \bar{\lambda}_i} \geq 10,$$

is satisfied, which means a “big” jump between $\lambda_{\hat{r}}$ and $\lambda_{\hat{r}+1}$, then we reduce d to \hat{r} , and this adjustment is performed only once.

5. Theoretical Analysis and Applications

In this section, we will present several theoretical properties of Algorithm 1. First, we provide the equivalent relationship analysis for our iterative solving scheme and the one in [38], as shown by the following theorem.

Theorem 7. Let (U_k^*, V_k^*, S_k^*) be the solution of the subproblems (11), (12) and (13) at the k -th iteration, respectively, $Y_k^* = Y_{k-1}^* + \alpha_{k-1}(D - U_k^*(V_k^*)^T - S_k^*)$, and (U_k, V_k, S_k, Y_k) be generated by Algorithm 1 at the k -th iteration, $(k = 1, \dots, T)$. Then

1. $\exists O_k \in \mathcal{O} = \{M \in \mathbb{R}^{d \times d} | M^T M = I\}$ such that $U_k^* = U_k O_k$ and $V_k^* = V_k O_k$.
2. $U_k^*(V_k^*)^T = U_k V_k^T$, $\|V_k^*\|_* = \|V_k\|_*$, $S_k^* = S_k$, and $Y_k^* = Y_k$.

Remark: The proof of this theorem can be found in APPENDIX D. Since the Lagrange function (10) is determined by the product UV^T , V , S and Y , the different values of U and V are essentially equivalent as long as the same product UV^T and $\|V\|_* = \|V^*\|_*$. Meanwhile, our scheme replaces SVD by the QR decomposition, and can avoid the SVD computation for solving the optimization problem with the orthogonal constraint.

5.1. Convergence Analysis

The global convergence of our derived algorithm is guaranteed, as shown in the following lemmas and theorems.

Lemma 8. Let (U_k, V_k, S_k) be a sequence generated by Algorithm 1, then we have the following conclusions:

1. (U_k, V_k, S_k) approaches to a feasible solution, i.e., $\lim_{k \rightarrow \infty} \|D - U_k V_k^T - S_k\|_F = 0$.
2. Both sequences $U_k V_k^T$ and S_k are Cauchy sequences.

The detailed proofs of this lemma, the following lemma and theorems can be found in APPENDIX E. Lemma 8 ensures only that the feasibility of each solution has been assessed. In this paper, we want to show that it is possible to prove the local optimality of the solution produced by Algorithm 1. Let k^* be the number of iterations needed by Algorithm 1 to stop, and (U^*, V^*, S^*) be defined by

$$U^* = U_{k^*+1}, \quad V^* = V_{k^*+1}, \quad S^* = S_{k^*+1}.$$

In addition, let Y^* (resp. \widehat{Y}^*) denote the Lagrange multiplier Y_{k^*+1} (resp. \widehat{Y}_{k^*+1}) associated with (U^*, V^*, S^*) , i.e., $Y^* = Y_{k^*+1}$, $\widehat{Y}^* = \widehat{Y}_{k^*+1}$, where $\widehat{Y}_{k^*+1} = Y_{k^*} + \alpha_{k^*}(D - U_{k^*+1} V_{k^*+1}^T - S_{k^*})$.

Lemma 9. For the solution (U^*, V^*, S^*) generated by Algorithm 1, then we have the following conclusion:

$$\|\mathcal{P}_\Omega(S)\|_1 + \lambda \|V\|_* \geq \|\mathcal{P}_\Omega(S^*)\|_1 + \lambda \|V^*\|_* + \langle \widehat{Y}^* - Y^*, UV^T - U^*(V^*)^T \rangle - mn\varepsilon$$

holds for any feasible solution (U, V, S) to (9).

To reach the global optimality of (9) based on the above lemma, it is required to show that the term $\langle \widehat{Y}^* - Y^*, UV^T - U^*(V^*)^T \rangle$ diminishes. Since

$$\|Y^* - \widehat{Y}^*\|_2 \leq \sqrt{mn} \|Y^* - \widehat{Y}^*\|_\infty,$$

and by Lemma 13 (Please see APPENDIX E), we have

$$\|Y^* - \widehat{Y}^*\|_\infty = \|\mathcal{P}_\Omega(Y^*) - \widehat{Y}^*\|_\infty \leq \|\mathcal{P}_\Omega(Y^*)\|_\infty + \|\widehat{Y}^*\|_\infty \leq 1 + \lambda,$$

which means that $\|Y^* - \widehat{Y}^*\|_\infty$ is bounded. By setting the parameter ρ to be relatively small as in [38], $\|Y^* - \widehat{Y}^*\|_\infty$ is small, which means that $\|Y^* - \widehat{Y}^*\|_2$ is also small. Let $\varepsilon_1 = \|Y^* - \widehat{Y}^*\|_2$, then we have the following theorems.

Theorem 10. Let f^g be the globally optimal objective function value of (9), and $f^* = \|\mathcal{P}_\Omega(S^*)\|_1 + \lambda\|V^*\|_*$ be the objective function value generated by Algorithm 1. We have that

$$f^* \leq f^g + c_1\varepsilon_1 + mn\varepsilon,$$

where c_1 is a constant defined by

$$c_1 = \frac{mn}{\lambda} \|\mathcal{P}_\Omega(D)\|_F \left(\frac{\rho(1+\rho)}{\rho-1} + \frac{1}{2\rho^{k^*}} \right) + \frac{\|\mathcal{P}_\Omega(D)\|_1}{\lambda}.$$

Theorem 11. Suppose (L^0, S^0) is an optimal solution to the RMC problem (5), $\text{rank}(L^0) = r$ and $f^0 = \|\mathcal{P}_\Omega(S^0)\|_1 + \lambda\|L^0\|_*$. Let $f^* = \|\mathcal{P}_\Omega(S^*)\|_1 + \lambda\|U^*V^*\|_*$ be the objective function value generated by Algorithm 1 with parameter $d > 0$. We have that

$$f^0 \leq f^* \leq f^0 + c_1\varepsilon_1 + mn\varepsilon + (\sqrt{mn} - \lambda)\sigma_{d+1} \max(r - d, 0),$$

where $\sigma_1 \geq \sigma_2 \geq \dots$ are the singular values of L^0 .

Since the rank parameter d is set to be higher than the rank of the optimal solution to the RMC problem (5), i.e., $d \geq r$, Theorem 11 directly concludes that

$$f^0 \leq f^* \leq f^0 + c_1\varepsilon_1 + mn\varepsilon.$$

Moreover, the value of ε can be set to be arbitrarily small, and the second term involving ε_1 diminishes. Hence, for the solution (U^*, V^*, S^*) generated by Algorithm 1, a solution to the RMC problem (5) can be achieved by computing $L^* = U^*(V^*)^T$.

5.2. Complexity Analysis

We also discuss the time complexity of our RBF algorithm. For the RMC problem (7), the main running time of our RBF algorithm is consumed by performing SVD on the small matrix of size $n \times d$, the QR decomposition of the matrix $P_k V_k$, and some matrix multiplications. In (17), the time complexity of performing SVD is $O(d^2n)$. The time complexity of QR decomposition and matrix multiplications is $O(d^2m + mnd)$. The total time complexity of our RBF algorithm for solving both problems (3) and (7) is $O(t(d^2n + d^2m + mnd))$ (usually $d \ll n \leq m$), where t is the number of iterations.

5.3. Applications of Matrix Completion

As our RBF framework introduced for robust matrix factorization is general, there are many possible extensions of our methodology. In this section, we outline a novel result and methodology for one extension we consider most important: low-rank matrix completion. The space limit refrains us from fully describing each development, but we try to give readers enough details to understand and use each of these applications.

By introducing an auxiliary variable L , the low-rank matrix completion problem can be written into the following form,

$$\begin{aligned} \min_{U, V, L} \quad & \frac{1}{2} \|\mathcal{P}_\Omega(D) - \mathcal{P}_\Omega(L)\|_F^2 + \lambda\|V\|_*, \\ \text{s.t.}, \quad & L = UV^T, U^T U = I. \end{aligned} \tag{28}$$

Similar to Algorithm 1, we can present an efficient ADMM scheme to solve the matrix completion problem (28). This algorithm can also be easily used to solve the low-rank matrix factorization problem, where all entries of the given matrix are observed.

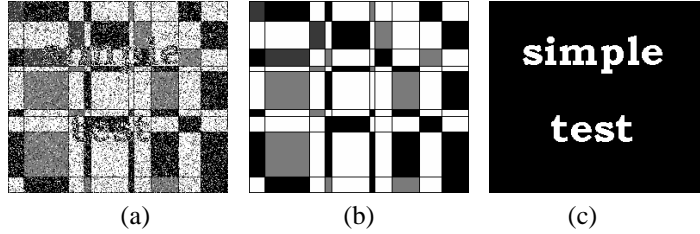


Figure 2: Image used in text removal experiment: (a) Input image; (b) Original image; (c) Outlier mask.

6. Experimental Evaluation

We now evaluate the effectiveness and efficiency of our RBF method for RMC and CPCP problems such as text removal, background modeling, face reconstruction, and collaborative filtering. We ran experiments on an Intel(R) Core (TM) i5-4570 (3.20 GHz) PC running Windows 7 with 8GB main memory.

6.1. Text Removal

We first conduct an experiment by considering a simulated task on artificially generated data, whose goal is to remove some generated text from an image. The ground-truth image is of size 256×222 with rank equal to 10 for the data matrix. we then add to the image a short phase in text form which plays the role of outliers. Fig. 2 shows the image together with the clean image and outliers mask. For fairness, we set the rank of all the algorithms to 20, which is two times the true rank of the underlying matrix. The input data are generated by setting 30% of the randomly selected pixels of the image as missing entries. We compare our RBF method with the state-of-the-art methods, including PCP [9], SpaRCS¹ [6], RegL1² [11] and BF-ALM [12]. We set the regularization parameter $\lambda = \sqrt{\max(m, n)}$ for RegL1 and RBF, and the stopping tolerance $\varepsilon = 10^{-4}$ for all algorithms in this section.

The results obtained by different methods are visually shown in Fig. 3, where the outlier detection accuracy (the score Area Under the receiver operating characteristic Curve, AUC) and the error of low-rank component recovery (i.e., $\|D-L\|_F/\|D\|_F$, where D and L denote the ground-truth image matrix and the recovered image matrix, respectively) are also presented. As far as low-rank matrix recovery is concerned, these RMC methods including SpaRCS, RegL1, BF-ALM and RBF, outperform PCP, not only visually but also quantitatively. For outlier detection, it can be seen that our RBF method significantly performs better than the other methods. In short, RBF significantly outperforms PCP, RegL1, BF-ALM and SpaRCS in terms of both low-rank matrix recovery and spare outlier identification. Moreover, the running time of PCP, SpaRCS, RegL1, BF-ALM and RBF is 36.25sec, 15.68sec, 26.85sec, 6.36sec and 0.87sec, respectively.

We further evaluate the robustness of our RBF method with respect to the regularization parameter λ and the given rank variations. We conduct some experiments on the artificially generated data, and illustrate the outlier detection accuracy (AUC) and the error (Error) of low-rank component recovery of PCP, SpaRCS, RegL1 and our RBF method, where the given rank of SpaRCS, RegL1 and our RBF method is chosen from $\{20, 25, \dots, 60\}$, and the regularization

¹<http://www.ece.rice.edu/~aew2/sparcs.html>

²<https://sites.google.com/site/yinqiangzheng/>

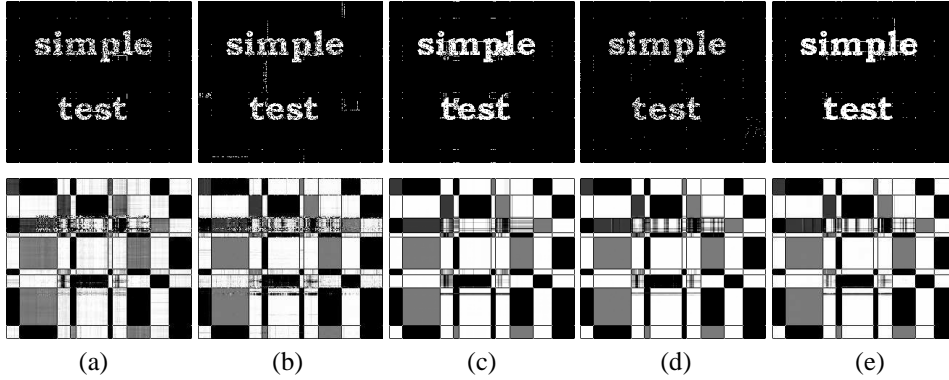


Figure 3: Text removal results. The first row shows the foreground masks and the second row shows the recovered background images: (a) PCP (AUC: 0.8558; Error: 0.2516); (b) SpaRCS (AUC: 0.8665; Error: 0.2416); (c) RegL1 (AUC: 0.8792; Error: 0.2291); (d) BF-ALM (AUC: 0.8568; Error: 0.2435); (e) RBF (AUC: 0.9227; Error: 0.1844).

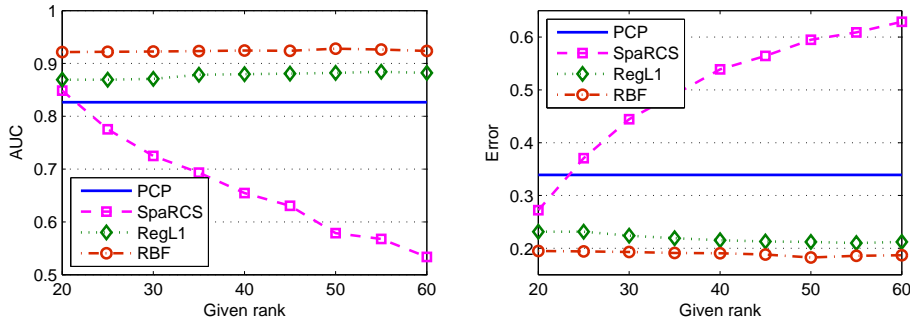


Figure 4: Comparison of PCP, SpaRCS, RegL1 and our RBF method in terms of AUC (Left) and Error (Right) on the artificially generated data with varying ranks.

parameter λ of PCP, RegL1 and RBF is chosen from the grid $\{1, 2.5, 5, 7.5, 10, 25, 50, 75, 100\}$. Notice that because BF-ALM and RegL1 achieve very similar results, we do not provide the results of the former in the following. The average AUC and Error results of 10 independent runs are shown in Figs. 4 and 5, from which we can see that our RBF method performs much more robust than SpaRCS and RegL1 with respect to the given rank. Moreover, our RBF method is much more robust than PCP and RegL1 against the regularization parameter λ .

6.2. Background Modeling

In this experiment we test our RBF method on real surveillance videos for object detection and background subtraction as a RPCA plus matrix completion problem. Background modeling is a crucial task for motion segmentation in surveillance videos. A video sequence satisfies the low-rank and sparse structures, because the background of all the frames is controlled by few factors and hence exhibits low-rank property, and the foreground is detected by identifying spatially localized sparse residuals [5, 9, 43]. We test our RBF method on four color surveillance

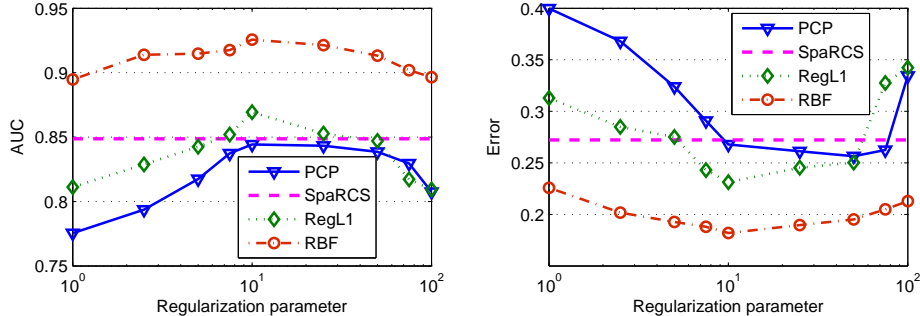


Figure 5: Comparison of PCP, SpaRCS, RegL1 and our RBF method in terms of AUC (Left) and Error (Right) on the artificially generated data with varying regularization parameters.

videos: Bootstrap, Lobby, Hall and Mall databases³. The data matrix D consists of the first 400 frames of size 144×176 . Since all the original videos have colors, we first reshape every frame of the video into a long column vector and then collect all the columns into a data matrix D with size of 76032×400 . Moreover, the input data is generated by setting 10% of the randomly selected pixels of each frame as missing entries.

Fig. 6 illustrates the background extraction results on the Bootstrap data set, where the first and fourth columns represent the input images with missing data, the second and fifth columns show the low-rank recoveries, and the third and sixth columns show the sparse components. It is clear that the background can be effectively extracted by our RBF method, RegL1 and GRASTA⁴ [44]. Notice that SpaRCS could not yield experimental results on these databases because they ran out of memory. Moreover, we can see that the decomposition results of our RBF method, especially the recovered low-rank components, are slightly better than that of RegL1 and GRASTA. We also report the running time in Table 1, from which we can see that RBF is more than 3 times faster than GRASTA and more than 2 times faster than RegL1. This further shows that our RBF method has very good scalability and can address large-scale problems.

Table 1: Comparison of time costs in CPU seconds of GRASTA, RegL1 and RBF on background modeling data sets.

Datasets	Sizes	GRASTA	RegL1	RBF
Bootstrap	$57,600 \times 400$	153.65	93.17	38.32
Lobby	$61,440 \times 400$	187.43	139.83	50.08
Hall	$76,032 \times 400$	315.11	153.45	67.73
Mall	$245,760 \times 200$	493.92	—	94.59

6.3. Face Reconstruction

We also test our RBF method for the face reconstruction problems with the incomplete and corrupted face data or a small set of linear measurements y as in [1], respectively. The face database used here is a part of Extended Yale Face Database B [28] with the large corruptions.

³<http://perception.i2r.a-star.edu.sg/bkmodel/bkindex>

⁴<https://sites.google.com/site/hejunzz/grasta>

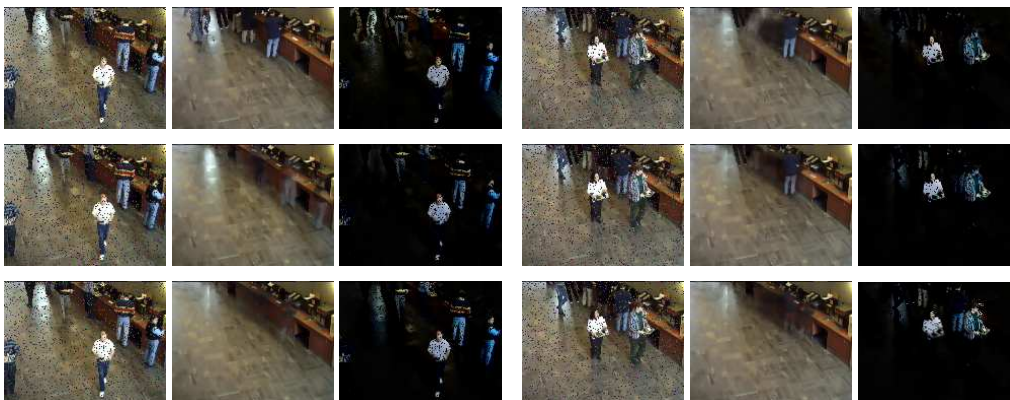


Figure 6: Background extraction results of different algorithms on the Bootstrap data set, where the first, second and last rows show the recovered low-rank and sparse images by GRASTA, RegL1 and RBF, respectively.

The face images can often be decomposed as a low-rank part, capturing the face appearances under different illuminations, and a sparse component, representing varying illumination conditions and heavily “shadows”. The resolution of all images is 192×168 and the pixel values are normalized to $[0, 1]$, then the pixel values are used to form data vectors of dimension 32,256. The input data are generated by setting 40% of the randomly selected pixels of each image as missing entries.

Fig. 7 shows some original and reconstructed images by RBF, PCP, RegL1 and CWM⁵ [27], where the average computational time of all these algorithms on each people’s faces is presented. It can be observed that RBF performs better than the other methods not only visually but also efficiently, and effectively eliminates the heavy noise and “shadows” and simultaneously completes the missing entries. In other words, RBF can achieve the latent features underlying the original images regardless of the observed data corrupted by outliers or missing values.

Moreover, we implement a challenging problem to recover face images from incomplete line measurements. Considering the computational burden of the projection operator \mathcal{P}_Q , we resize the original images into 42×48 and normalize the raw pixel values to form data vectors of dimension 2016. Following [1], the input data is $\mathcal{P}_Q(D)$, where Q is a subspace generated randomly with the dimension $0.75mn$.

Fig. 8 illustrates some reconstructed images by CPCP [1] and RBF, respectively. It is clear that both CPCP and RBF effectively remove “shadows” from faces images and simultaneously successfully recover both low-rank and sparse components from the reduced measurements.

6.4. Collaborative Filtering

Collaborative filtering is a technique used by some recommender systems [45, 46]. One of the main purposes is to predict the unknown preference of a user on a set of unrated items, according to other similar users or similar items. In order to evaluate our RBF method, some matrix completion experiments are conducted on three widely used recommendation system data sets: MovieLens100K with 100K ratings, MovieLens1M (ML-1M) with 1M ratings and MovieLens10M (ML-10M) with 10M ratings. We randomly split these data sets to training and testing

⁵<http://www4.comp.polyu.edu.hk/~cslzhang/papers.htm>



Figure 7: Face recovery results by these algorithms. From left column to right column: Input corrupted images (black pixels denote missing entries), original images, reconstruction results by PCP (1020.69sec), CWM (1830.18sec), RegL1 (2416.85sec) and RBF (52.73sec).

sets such that the ratio of the training set to testing set is 9:1, and the experimental results are reported over 10 independent runs. We also compare our RBF method with APG⁷ [47], Soft-Impute⁶ [48], OptSpace⁷ [42] and LMaFit⁸ [36], and two state-of-the-art manifold optimization methods: ScGrass⁹ [49] and RTRMC¹⁰ [50]. All other parameters are set to their default values for all compared algorithms. We use the Root Mean Squared Error (RMSE) as the evaluation measure, which is defined as

$$\text{RMSE} = \sqrt{\frac{1}{|\Omega|} \sum_{(i,j) \in \Omega} (D_{ij} - L_{ij})^2},$$

where $|\Omega|$ is the total number of ratings in the testing set, L_{ij} denotes the ground-truth rating of user i for item j , and D_{ij} denotes the corresponding predicted rating.

The average RMSE on these three data sets is reported over 10 independent runs and is shown in Table 2. From the results shown in Table 2, we can see that, for some fixed ranks, most matrix factorization methods including ScGrass, RTRMC, LMaFit and our RBF method, except OptSpace, usually perform better than the two convex trace norm minimization methods, APG and Soft-Impute. Moreover, our bilinear factorization method with trace norm regularization

⁷<http://www.math.nus.edu.sg/~mattohkc/NNLS.html>

⁶<http://www.stat.columbia.edu/~rahulm/software.html>

⁷<http://web.engr.illinois.edu/~swoh/software/optspace/>

⁸<http://lmafit.blogs.rice.edu/>

⁹<http://www-users.cs.umn.edu/~thango/>

¹⁰<http://perso.uclouvain.be/nicolas.boumal/RTRMC/>

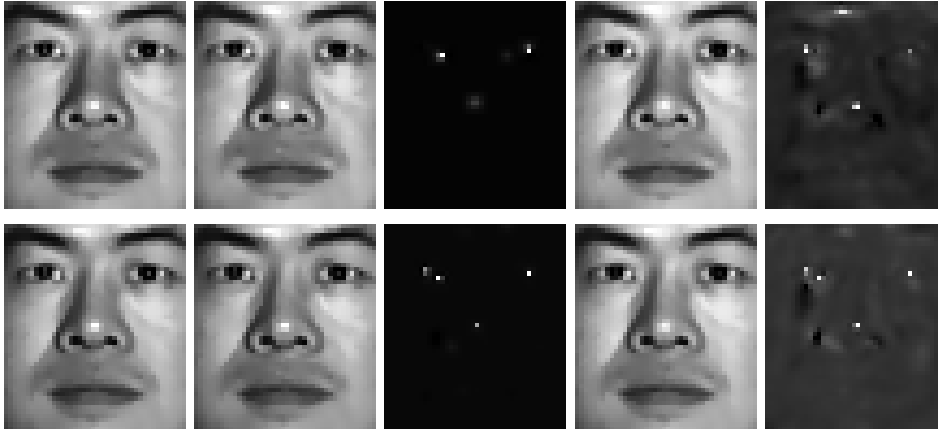


Figure 8: Face reconstruction results by CPCP and RBF, where the first column show the original images, the second and third columns show the low-rank and sparse components obtained by CPCP, while the last two columns show the low-rank and sparse components obtained by RBF.

Table 2: RMSE of different methods on three data sets: MovieLens100K, MovieLens1M and MovieLens10M.

Methods	MovieLens100K			MovieLens1M			MovieLens10M		
APG	1.2142			1.1528			0.8583		
Soft-Impute	1.0489			0.9058			0.8615		
OptSpace	0.9411			0.9071			1.1357		
Ranks	5	6	7	5	6	7	5	6	7
ScGrass	0.9647	0.9809	0.9945	0.8847	0.8852	0.8936	0.8359	0.8290	0.8247
RTRMC	0.9837	1.0617	1.1642	0.8875	0.8893	0.8960	0.8463	0.8442	0.8386
LMaFit	0.9468	0.9540	0.9568	0.8918	0.8920	0.8853	0.8576	0.8530	0.8423
RBF	0.9393	0.9513	0.9485	0.8672	0.8624	0.8591	0.8193	0.8159	0.8110

consistently outperforms the other matrix factorization methods including OptSpace, ScGrass, RTRMC and LMaFit, and the two trace norm minimization methods, APG and Soft-Impute. This confirms that our robust bilinear factorization model with trace norm regularization is reasonable.

Furthermore, we also analyze the robustness of our RBF method with respect to its parameter changes: the given rank and the regularization parameter λ on the MovieLens1M data set, as shown in Fig. 9, from which we can see that our RBF method is very robust against its parameter variations. For comparison, we also show the results of some related methods: ScGrass and LMaFit, OptSpace and RTRMC with varying ranks or different regularization parameters in Fig. 9. It is clear that, by increasing the number of the given ranks, the RMSE of ScGrass and LMaFit, RTRMC becomes dramatically increases, while that of our RBF method increase slightly. This further confirms that our bilinear matrix factorization model with trace norm regularization can significantly reduce the over-fitting problems of matrix factorization. ScGrass, RTRMC and OptSpace all have their spectral regularization models, respectively (for example, the formulation for OptSpace is $\min_{U,S,V} (1/2) \|\mathcal{P}_\Omega(USV^T - D)\|_F^2 + \lambda \|S\|_F^2$.) We can see that our RBF method performs more robust than OptSpace, ScGrass and RTRMC in terms of the regularization parameter λ . Moreover, our RBF method is easily used to incorporate side-information as in [51, 52, 8, 53, 54].

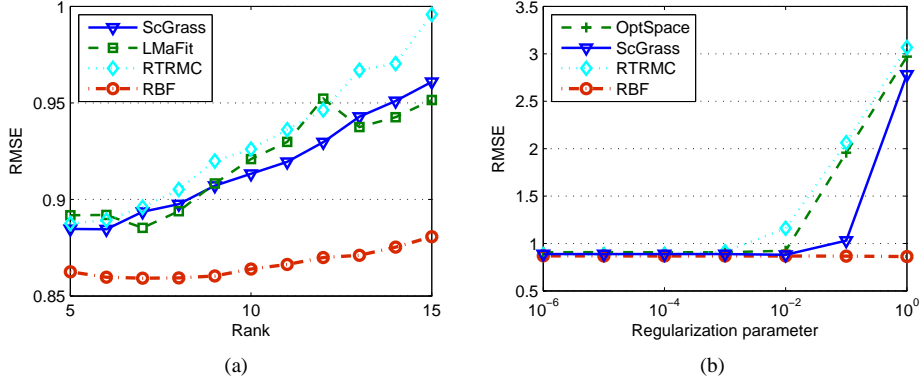


Figure 9: Results of our RBF method, ScGrass, LMaFit, and OptSpace against their parameters: (a) Rank and (b) Regularization parameter λ .

7. CONCLUSIONS

In this paper, we proposed a scalable robust bilinear structured factorization (RBF) framework for RMC and CPCP problems. Unlike existing robust low-rank matrix factorization methods, the proposed RBF method can not only address large-scale RMC problems, but can also solve low-rank and sparse matrix decomposition problems with incomplete or corrupted observations. To this end, we first presented two smaller-scale matrix trace norm regularized models for RMC and CPCP problems, respectively. Then we developed an efficient ADMM algorithm to solve both RMC and RPCA problems, and analyzed the suboptimality of the solution produced by our algorithm. Finally, we extended our algorithm to solve CPCP problems. Experimental results on real-world data sets demonstrated the superior performance of our RBF method in comparison with the state-of-the-art methods in terms of both efficiency and effectiveness.

APPENDIX A: Proof of Lemma 2

Proof. Let (L^*, S^*) be the optimal solution of (4), $g(L, S) = \|S\|_1 + \lambda \|L\|_*$ and $\Gamma = \{(L, S) \mid \mathcal{P}_\Omega(D) = \mathcal{P}_\Omega(L + S)\}$, then we use contradiction to prove that $\mathcal{P}_{\Omega^c}(S^*) = \mathbf{0}$.

We first assume $\mathcal{P}_{\Omega^c}(S^*) \neq \mathbf{0}$. Let \tilde{S}^* be $(\tilde{S}^*)_\Omega = (S^*)_\Omega$ and $(\tilde{S}^*)_{\Omega^c} = \mathbf{0}$, then we have $(L^*, \tilde{S}^*) \in \Gamma$ and $g(L^*, \tilde{S}^*) \leq g(L^*, S^*)$ that leads to a contradiction. Thus, $\mathcal{P}_{\Omega^c}(S^*) = \mathbf{0}$. Therefore, (L^*, S^*) is also the optimal solution of (5). \square

APPENDIX B: Proof of Lemma 3

Proof. Let the SVD of V^T be $V^T = \hat{U}\hat{\Sigma}\hat{V}^T$, then $UV^T = (U\hat{U})\hat{\Sigma}\hat{V}^T$. As $(U\hat{U})^T(U\hat{U}) = I$, $(U\hat{U})\hat{\Sigma}\hat{V}^T$ is actually an SVD of UV^T . According to the definition of the trace norm, we have $\|V\|_* = \|V^T\|_* = \text{tr}(\hat{\Sigma}) = \|UV^T\|_*$. \square

APPENDIX C: Proof of Theorem 4

Proof. If we know that (L^*, S^*) is a solution for the optimization problem (5), it is also a solution to

$$\begin{aligned} & \min_{L, S, \text{rank}(L)=r} \|\mathcal{P}_\Omega(S)\|_1 + \lambda \|L\|_*, \\ & \text{s.t.}, \mathcal{P}_\Omega(D) = \mathcal{P}_\Omega(L + S), \mathcal{P}_{\Omega^c}(S) = \mathbf{0}. \end{aligned}$$

Since for any (L, S) with $\text{rank}(L) = r$, we can find $U \in \mathbb{R}^{m \times d}$ and $V \in \mathbb{R}^{n \times d}$ satisfying $UV^T = L$ and $\mathcal{P}_\Omega(D - UV^T) = \mathcal{P}_\Omega(S)$, where $d \geq r$. Moreover, according to Lemma 3, we have

$$\begin{aligned} & \min_{U, V, S} \|\mathcal{P}_\Omega(S)\|_1 + \lambda \|V\|_* \\ & \text{s.t.}, \mathcal{P}_\Omega(D) = \mathcal{P}_\Omega(UV^T + S), U^T U = I, \\ & = \min_{U, V, S} \|\mathcal{P}_\Omega(S)\|_1 + \lambda \|UV^T\|_* \\ & \text{s.t.}, \mathcal{P}_\Omega(D) = \mathcal{P}_\Omega(UV^T + S), \\ & = \min_{L, S, \text{rank}(L)=r} \|\mathcal{P}_\Omega(S)\|_1 + \lambda \|L\|_* \\ & \text{s.t.}, \mathcal{P}_\Omega(D) = \mathcal{P}_\Omega(L + S), \end{aligned}$$

where $\mathcal{P}_{\Omega^c}(S) = \mathbf{0}$. This completes the proof. \square

APPENDIX D: Proof of Theorem 7

Proof. We will prove the statement in Theorem 7 using mathematical induction.

1. While $k = 1$, and following [37], then the optimal solution to the problem (14) is given by

$$U_1^* = \widetilde{U}_1 \widetilde{V}_1^T,$$

where the skinny SVD of $P_0^* V_0^*$ is $P_0^* V_0^* = \widetilde{U}_1 \widetilde{\Sigma}_1 \widetilde{V}_1^T$.

By Algorithm 1, and with the same initial values, i.e., $U_0^* = U_0$, $V_0^* = V_0$, $S_0^* = S_0$ and $P_0^* = P_0$, then we have

$$U_1 = Q, \quad \text{QR}(P_0 V_0) = \text{QR}(P_0^* V_0^*) = QR.$$

Hence, it can be easily verified that $\exists O_1 \in \mathcal{N}$ satisfies $U_1^* = U_1 O_1$, where $\mathcal{N} = \{A \in \mathbb{R}^{d \times d}, A^T A = I, A A^T = I\}$.

By the iteration step (19), we have

$$\begin{aligned} V_1^* &= \text{SVT}_{\lambda/\alpha_k}((P_0^*)^T U_1^*) \\ &= \text{SVT}_{\lambda/\alpha_k}((P_0^*)^T U_1 O_1) \\ &= \text{SVT}_{\lambda/\alpha_k}((P_0^*)^T U_1) O_1 \\ &= V_1 O_1. \end{aligned}$$

Thus, $U_1^*(V_1^*)^T = U_1 V_1^T$. Furthermore, we have

$$S_1^* = S_1, P_1^* = P_1 \text{ and } Y_1^* = Y_1.$$

2. While $k > 1$, the result of Theorem 7 holds at the $(k-1)$ -th iteration, then following [37] and [38], U_k^* is updated by

$$U_k^* = \widetilde{U}_k \widetilde{V}_k^T,$$

where the skinny SVD of $P_{k-1}^* V_{k-1}^*$ is $P_{k-1}^* V_{k-1}^* = \widetilde{U}_k \widetilde{\Sigma}_k \widetilde{V}_k^T$.

By $P_{k-1}^* V_{k-1}^* = P_{k-1}^* V_{k-1} O_{k-1}$, and according to (15), then $\exists O_k \in \mathcal{N}$ satisfies $U_k^* = U_k O_k$. Furthermore, we have

$$\begin{aligned} U_k^*(V_k^*)^T &= U_k^* \text{SVT}_{\lambda/\alpha_{k-1}}((U_k^*)^T P_{k-1}^*) \\ &= \text{SVT}_{\lambda/\alpha_k}(U_k^*(U_k^*)^T P_{k-1}^*) \\ &= \text{SVT}_{\lambda/\alpha_k}(U_k(U_k)^T P_{k-1}) \\ &= U_k V_k^T, \end{aligned}$$

and $V_k^* = V_k O_k$, $S_k^* = S_k$, $P_k^* = P_k$ and $Y_k^* = Y_k$.

Since $V_k^* = V_k O_k$, we also have $\|V_k^*\|_* = \|V_k\|_*$.

This completes the proof. \square

APPENDIX E

The proof sketch of Lemma 8 is similar to the one in [38]. We first prove that the boundedness of multipliers and some variables of Algorithm 1, and then analyze the convergence of Algorithm 1. To prove the boundedness, we first give the following lemmas.

Lemma 12. *Let \mathcal{X} be a real Hilbert space endowed with an inner product $\langle \cdot, \cdot \rangle$ and a corresponding norm $\|\cdot\|$ (the nuclear norm or the l_1 norm), and $y \in \partial\|x\|$, where $\partial\|\cdot\|$ denotes the subgradient. Then $\|y\|^* = 1$ if $x \neq 0$, and $\|y\|^* \leq 1$ if $x = 0$, where $\|\cdot\|^*$ is the dual norm of the norm $\|\cdot\|$.*

Lemma 13. *Let $Y_{k+1} = Y_k + \alpha_k(D - U_{k+1} V_{k+1}^T - S_{k+1})$, $\widehat{Y}_{k+1} = Y_k + \alpha_k(D - U_{k+1} V_{k+1}^T - S_k)$ and $\widetilde{Y}_{k+1} = Y_k + \alpha_k(D - U_{k+1}^* V_k^T - S_k)$, where U_{k+1}^* is the solution of the problem (14). Then the sequences $\{Y_k\}$, $\{\widehat{Y}_k\}$, $\{\widetilde{Y}_k\}$, $\{V_k\}$ and $\{S_k\}$ produced by Algorithm 1 are all bounded.*

Proof. By the optimality condition of the problem (20) with respect to S_{k+1} , we have that

$$0 \in \partial_{(S_{k+1})\Omega} \mathcal{L}_{\alpha_k}(U_{k+1}, V_{k+1}, S_{k+1}, Y_k),$$

and

$$\mathcal{P}_\Omega(Y_k + \alpha_k(D - U_{k+1} V_{k+1}^T - S_{k+1})) \in \partial\|\mathcal{P}_\Omega(S_{k+1})\|_1,$$

i.e.,

$$\mathcal{P}_\Omega(Y_{k+1}) \in \partial\|\mathcal{P}_\Omega(S_{k+1})\|_1. \quad (29)$$

Furthermore, substituting $Y_{k+1} = Y_k + \alpha_k(D - U_{k+1} V_{k+1}^T - S_{k+1})$ into (23), we have

$$\mathcal{P}_{\Omega^c}(Y_{k+1}) = \mathbf{0}.$$

By Lemma 12, we have

$$\|Y_{k+1}\|_\infty = \|\mathcal{P}_\Omega(Y_{k+1})\|_\infty \leq 1. \quad (30)$$

Thus, the sequence $\{\widehat{Y}_k\}$ is bounded.

From the iteration procedure of Algorithm 1, we have that

$$\begin{aligned} & \mathcal{L}_{\alpha_k}(U_{k+1}, V_{k+1}, S_{k+1}, Y_k) \\ & \leq \mathcal{L}_{\alpha_k}(U_{k+1}, V_{k+1}, S_k, Y_k) \leq \mathcal{L}_{\alpha_k}(U_k, V_k, S_k, Y_k) \\ & = \mathcal{L}_{\alpha_{k-1}}(U_k, V_k, S_k, Y_{k-1}) + \beta_k \|Y_k - Y_{k-1}\|_F^2. \end{aligned}$$

where $\beta_k = \frac{1}{2}\alpha_{k-1}^{-2}(\alpha_{k-1} + \alpha_k)$ and $\alpha_k = \rho\alpha_{k-1}$.

Hence,

$$\sum_{k=1}^{\infty} 2\alpha_{k-1}^{-2}(\alpha_{k-1} + \alpha_k) = \frac{\rho(\rho + 1)}{2\alpha_0(\rho - 1)} < \infty. \quad (31)$$

Thus, $\{\mathcal{L}_{\alpha_{k-1}}(U_k, V_k, S_k, Y_{k-1})\}$ is upper bounded due to the boundedness of $\{Y_k\}$. Then

$$\begin{aligned} & \lambda\|V_k\|_* + \|\mathcal{P}_{\Omega}(S_k)\|_1 \\ & = \mathcal{L}_{\alpha_{k-1}}(U_k, V_k, S_k, Y_{k-1}) - \frac{1}{2}\alpha_{k-1}^{-1}(\|Y_k\|_F^2 - \|Y_{k-1}\|_F^2), \end{aligned}$$

is upper bounded, i.e., $\{V_k\}$ and $\{S_k\}$ are bounded, and $\{U_k V_k^T\}$ is also bounded.

We next prove that $\{\widetilde{Y}_k\}$ is bounded. Let U_{k+1}^* denote the solution of the subproblem (14). By the optimality of U_{k+1}^* , then we have

$$\|Y_k + \alpha_k(D - U_{k+1}^* V_k^T)\|_F^2 \leq \|Y_k + \alpha_k(D - U_k V_k^T - S_k)\|_F^2,$$

and by the definition of \widetilde{Y}_k , and $\alpha_{k+1} = \rho\alpha_k$, thus,

$$\|\widetilde{Y}_k\|_F^2 \leq \|(1 + \rho)Y_k - \rho Y_{k-1}\|_F^2.$$

By the boundedness of V_k and Y_k , then the sequence $\{\widetilde{Y}_k\}$ is bounded.

The optimality condition of the problem (16) with respect to V_{k+1} is rewritten as follows:

$$U_{k+1}^T \widehat{Y}_{k+1} \in \lambda \partial \|V_{k+1}^T\|_*. \quad (32)$$

By Lemma 12, we have that

$$\|U_{k+1}^T \widehat{Y}_{k+1}\|_2 \leq \lambda.$$

Thus, $U_{k+1}^T \widehat{Y}_{k+1}$ is bounded. Let U_{k+1}^\perp denote the orthogonal complement of U_{k+1} , i.e., $U_{k+1}^\perp U_{k+1} = \mathbf{0}$, and according to Theorem 7, then $\exists O_{k+1}$ satisfies $U_{k+1}^* = U_{k+1} O_{k+1}$, thus we have

$$\begin{aligned} & (U_{k+1}^\perp)^T \widehat{Y}_{k+1} \\ & = (U_{k+1}^\perp)^T (Y_k + \alpha_k(D - U_{k+1} V_{k+1}^T - S_k)) \\ & = (U_{k+1}^\perp)^T (Y_k + \alpha_k(D - U_{k+1} O_{k+1} V_k^T - S_k)) \\ & = (U_{k+1}^\perp)^T (Y_k + \alpha_k(D - U_{k+1}^* V_k^T - S_k)) \\ & = (U_{k+1}^\perp)^T \widetilde{Y}_k. \end{aligned}$$

Thus, $\{(U_{k+1}^\perp)^T \widehat{Y}_{k+1}\}$ is bounded due to the boundedness of $\{\widetilde{Y}_k\}$. Then we have

$$\|\widehat{Y}_{k+1}\|_2 = \|U_{k+1}^T \widehat{Y}_{k+1} + (U_{k+1}^\perp)^T \widehat{Y}_{k+1}\|_2 \leq \|U_{k+1}^T \widehat{Y}_{k+1}\|_2 + \|(U_{k+1}^\perp)^T \widehat{Y}_{k+1}\|_2.$$

Since both $U_{k+1}^T \widehat{Y}_{k+1}$ and $(U_{k+1}^\perp)^T \widehat{Y}_{k+1}$ are bounded, the sequence $\{\widehat{Y}_k\}$ is bounded. This completes the proof. \square

Proof of Lemma 8:

Proof. **1.** By $D - U_{k+1}V_{k+1}^T - S_{k+1} = \alpha_k^{-1}(Y_{k+1} - Y_k)$, the boundedness of $\{Y_k\}$ and $\lim_{k \rightarrow \infty} \alpha_k = \infty$, we have that

$$\lim_{k \rightarrow \infty} D - U_{k+1}V_{k+1}^T - S_{k+1} = 0.$$

Thus, (U_k, V_k, S_k) approaches to a feasible solution.

2. We prove that the sequences $\{S_k\}$ and $\{U_k V_k^T\}$ are Cauchy sequences.

By $\|S_{k+1} - S_k\| = \alpha_k^{-1} \|Y_{k+1} - Y_k\| = o(\alpha_k^{-1})$ and

$$\sum_{k=1}^{\infty} \alpha_k^{-1} = \frac{\rho}{\alpha_0(\rho - 1)} < \infty,$$

thus, $\{S_k\}$ is a Cauchy sequence, and it has a limit, S^* .

Similarly, $\{U_k V_k^T\}$ is also a Cauchy sequence, therefore it has a limit, $U^*(V^*)^T$.

This completes the proof. \square

To prove Lemma 9, we first give the following lemma in [38]:

Lemma 14. Let X, Y and Q be matrices of compatible dimensions. If Q obeys $Q^T Q = I$ and $Y \in \partial \|X\|_*$, then

$$QY \in \partial \|QX\|_*.$$

Proof of Lemma 9:

Proof. Let the skinny SVD of $P_k = D - S_k + Y_k/\alpha_k$ be $P_k = \widehat{U}_k \widehat{\Sigma}_k \widehat{V}_k^T$, then it can be calculated that

$$\text{QR}(P_k V_k) = \text{QR}(\widehat{U}_k \widehat{\Sigma}_k \widehat{V}_k^T V_k).$$

Let the full SVD of $\widehat{\Sigma}_k \widehat{V}_k^T V_k$ be $\widehat{\Sigma}_k \widehat{V}_k^T V_k = \widetilde{U} \widetilde{\Sigma} \widetilde{V}^T$ (note that \widetilde{U} and \widetilde{V} are orthogonal matrices), then it can be calculated that

$$\text{QR}(\widehat{U}_k \widehat{\Sigma}_k \widehat{V}_k^T V_k) = \text{QR}(\widehat{U}_k \widetilde{U} \widetilde{\Sigma} \widetilde{V}^T) = QR, \quad U_{k+1} = Q.$$

Then $\exists O$ and $O^T O = O O^T = I$ such that $U_{k+1} = \widehat{U}_k \widetilde{U} O$, which simply leads to

$$U_{k+1} U_{k+1}^T = \widehat{U}_k \widetilde{U} O O^T \widetilde{U}^T \widehat{U}_k^T = \widehat{U}_k \widehat{U}_k^T.$$

Hence,

$$\begin{aligned} \widehat{Y}_{k+1} - U_{k+1} U_{k+1}^T \widehat{Y}_{k+1} &= \mu_k ((D - S_k + Y_k/\mu_k) - U_{k+1} U_{k+1}^T (D - S_k + Y_k/\mu_k)) \\ &= \mu_k (\widehat{U}_k \widehat{\Sigma}_k \widehat{V}_k^T - U_{k+1} U_{k+1}^T \widehat{U}_k \widehat{\Sigma}_k \widehat{V}_k^T) \\ &= \mu_k (\widehat{U}_k \widehat{\Sigma}_k \widehat{V}_k^T - \widehat{U}_k \widetilde{U}^T \widetilde{U} \widehat{U}_k \widehat{\Sigma}_k \widehat{V}_k^T) = 0, \end{aligned}$$

i.e.,

$$\widehat{Y}_{k+1} = U_{k+1} U_{k+1}^T \widehat{Y}_{k+1}.$$

By (32) and Lemma 14, we have

$$U_{k+1}U_{k+1}^T\widehat{Y}_{k+1} \in \lambda\partial\|U_{k+1}V_{k+1}^T\|_*.$$

Thus, we have

$$\widehat{Y}_{k+1} \in \lambda\partial\|U_{k+1}V_{k+1}^T\|_* \text{ and } \mathcal{P}_\Omega(Y_{k+1}) \in \partial\|\mathcal{P}_\Omega(S_{k+1})\|_1, \forall k.$$

Since the above conclusion holds for any k , it naturally holds at (U^*, V^*, S^*) :

$$\widehat{Y}^* = \widehat{Y}_{k^*+1} \in \lambda\partial\|U^*(V^*)^T\|_* \text{ and } \mathcal{P}_\Omega(Y^*) = \mathcal{P}_\Omega(Y_{k^*+1}) \in \partial\|\mathcal{P}_\Omega(S^*)\|_1. \quad (33)$$

Given any feasible solution (U, V, S) to the problem (9), by the convexity of matrix norms and (33), and $\mathcal{P}_{\Omega^c}(Y^*) = \mathbf{0}$, it can be calculated that

$$\begin{aligned} \|\mathcal{P}_\Omega(S)\|_1 + \lambda\|V\|_* &= \|\mathcal{P}_\Omega(S)\|_1 + \lambda\|UV^T\|_* \\ &\geq \|\mathcal{P}_\Omega(S^*)\|_1 + \langle \mathcal{P}_\Omega(Y^*), \mathcal{P}_\Omega(S - S^*) \rangle + \lambda\|U^*(V^*)^T\|_* + \langle \widehat{Y}^*, UV^T - U^*(V^*)^T \rangle \\ &= \|\mathcal{P}_\Omega(S^*)\|_1 + \langle \mathcal{P}_\Omega(Y^*), S - S^* \rangle + \lambda\|U^*(V^*)^T\|_* + \langle \widehat{Y}^*, UV^T - U^*(V^*)^T \rangle \\ &= \|\mathcal{P}_\Omega(S^*)\|_1 + \lambda\|U^*(V^*)^T\|_* + \langle \mathcal{P}_\Omega(Y^*), UV^T + S - U^*(V^*)^T - S^* \rangle + \langle \widehat{Y}^* - \mathcal{P}_\Omega(Y^*), UV^T - U^*(V^*)^T \rangle \\ &= \|\mathcal{P}_\Omega(S^*)\|_1 + \lambda\|U^*(V^*)^T\|_* + \langle \mathcal{P}_\Omega(Y^*), UV^T + S - U^*(V^*)^T - S^* \rangle + \langle \widehat{Y}^* - Y^*, UV^T - U^*(V^*)^T \rangle. \end{aligned}$$

By Lemma 8 and $\|\mathcal{P}_\Omega(Y^*)\|_\infty \leq 1$, we have that $\|UV^T + S - U^*(V^*)^T - S^*\|_\infty = \|D - U^*(V^*)^T - S^*\|_\infty \leq \varepsilon$, which leads to

$$\begin{aligned} |\langle \mathcal{P}_\Omega(Y^*), UV^T + S - U^*(V^*)^T - S^* \rangle| &\leq \|\mathcal{P}_\Omega(Y^*)\|_\infty \|UV^T + S - U^*(V^*)^T - S^*\|_1 \\ &= \|\mathcal{P}_\Omega(Y^*)\|_\infty \|D - U^*(V^*)^T - S^*\|_1 \\ &\leq mn\|D - U^*(V^*)^T - S^*\|_\infty \leq mn\varepsilon. \end{aligned}$$

Hence,

$$\|\mathcal{P}_\Omega(S)\|_1 + \lambda\|V\|_* \geq \|\mathcal{P}_\Omega(S^*)\|_1 + \lambda\|V^*\|_* + \langle \widehat{Y}^* - Y^*, UV^T - U^*(V^*)^T \rangle - mn\varepsilon.$$

This completes the proof. \square

Proof of Theorem 10:

Proof. It is worth nothing that $(U, V = \mathbf{0}, S = D)$ is feasible to (9). Let (U^g, V^g, S^g) be a globally optimal solution to (9), then we have

$$\lambda\|V^g\|_* \leq \|\mathcal{P}_\Omega(S^g)\|_1 + \lambda\|V^g\|_* \leq \|D\|_1 = \|\mathcal{P}_\Omega(D)\|_1.$$

By the proof procedure of Lemma 13 and $\alpha_0 = \frac{1}{\|\mathcal{P}_\Omega(D)\|_F}$, we have that V^* is bounded by

$$\begin{aligned} \lambda\|V^*\|_* &\leq \|\mathcal{P}_\Omega(S^*)\|_1 + \lambda\|V^*\|_* \\ &\leq \mathcal{L}_{\alpha_{k^*}}(U_{k^*+1}, V_{k^*+1}, S_{k^*+1}, Y_{k^*}) + \frac{\|Y_{k^*}\|_F^2}{2\mu_{k^*}} \\ &\leq \frac{mn}{\alpha_0} \left(\frac{\rho(1+\rho)}{\rho-1} + \frac{1}{2\rho^{k^*}} \right) \\ &= mn\|\mathcal{P}_\Omega(D)\|_F \left(\frac{\rho(1+\rho)}{\rho-1} + \frac{1}{2\rho^{k^*}} \right). \end{aligned}$$

Thus,

$$\|U^g(V^g)^T - U^*(V^*)^T\|_* \leq \|V^g\|_* + \|V^*\|_* \leq c_1. \quad (34)$$

Note that $|\langle M, N \rangle| \leq \|M\|_2 \|N\|_*$ (please see [55]) holds for any matrices M and N . By Lemma 9 and (34), we have

$$\begin{aligned} f^g &= \|\mathcal{P}_\Omega(S^g)\|_1 + \lambda \|V^g\|_* \\ &\geq \|\mathcal{P}_\Omega(S^*)\|_1 + \lambda \|V^*\|_* + \langle \widehat{Y}^* - Y^*, U^g(V^g)^T - U^*(V^*)^T \rangle - mn\varepsilon \\ &\geq f^* - \|\widehat{Y}^* - Y^*\|_2 \|U^g(V^g)^T - U^*(V^*)^T\|_* - mn\varepsilon \\ &= f^* - \varepsilon_1 \|U^g(V^g)^T - U^*(V^*)^T\|_* - mn\varepsilon \\ &\geq f^* - c_1 \varepsilon_1 - mn\varepsilon. \end{aligned}$$

This completes the proof. \square

Proof of Theorem 11:

Proof. Let $L = U^*(V^*)^T$ and $S = S^*$, then (L, S) is a feasible solution to the RMC problem (5). By the convexity of the problem (5) and the optimality of (L^0, S^0) , it naturally follows that

$$f^0 \leq f^*.$$

Let $L^0 = U^0 \Sigma^0 (V^0)^T$ be the skinny SVD of L^0 . Construct $U' = U^0$, $(V')^T = \Sigma^0 (V^0)^T$ and $S' = S^0$. When $d \geq r$, we have

$$D = L^0 + S^0 = U^0 \Sigma^0 (V^0)^T + S^0 = U' (V')^T + S',$$

i.e., (U', V', S') is a feasible solution to the problem (9). By Theorem 10, it can be concluded that

$$f^* - c_1 \varepsilon_1 - mn\varepsilon \leq \lambda \|V'\|_* + \|\mathcal{P}_\Omega(S')\|_1 = \lambda \|\Sigma^0\|_* + \|\mathcal{P}_\Omega(S^0)\|_1 = f^0.$$

For $d \leq r$, we decompose the skinny SVD of L^0 as

$$L^0 = U_0 \Sigma_0 V_0^T + U_1 \Sigma_1 V_1^T,$$

where U_0, V_0 (resp. U_1, V_1) are the singular vectors associated with the d largest singular values (resp. the rest singular values smaller than or equal to σ_d). With these notations, we have a feasible solution to the problem (9) by constructing

$$U'' = U_0, (V'')^T = \Sigma_0 V_0^T \text{ and } S'' = D - U_0 \Sigma_0 V_0^T = S^0 + U_1 \Sigma_1 V_1^T.$$

By Theorem 10, it can be calculated that

$$\begin{aligned}
f^* - c_1 \varepsilon_1 - mn\varepsilon &\leq f^g \leq \lambda \|V''\|_* + \|\mathcal{P}_\Omega(S'')\|_1 \\
&\leq \lambda \|\Sigma_0\|_* + \|\mathcal{P}_\Omega(S^o + U_1 \Sigma_1 V_1^T)\|_1 \\
&\leq \lambda \|L^0\|_* - \lambda \|\Sigma_1\|_* + \|\mathcal{P}_\Omega(S^0)\|_1 + \|\mathcal{P}_\Omega(U_1 \Sigma_1 V_1^T)\|_1 \\
&\leq f^0 - \lambda \|\Sigma_1\|_* + \|U_1 \Sigma_1 V_1^T\|_1 \\
&\leq f^0 - \lambda \|\Sigma_1\|_* + \sqrt{mn} \|U_1 \Sigma_1 V_1^T\|_F \\
&\leq f^0 - \lambda \|\Sigma_1\|_* + \sqrt{mn} \|U_1 \Sigma_1 V_1^T\|_* \\
&\leq f^0 + (\sqrt{mn} - \lambda) \|\Sigma_1\|_* \\
&\leq f^0 + (\sqrt{mn} - \lambda) \sigma_{d+1}(r - d).
\end{aligned}$$

This completes the proof. \square

References

- [1] J. Wright, A. Ganesh, K. Min, Y. Ma, Compressive principal component pursuit, *Inform. Infer.* 2 (2013) 32–68.
- [2] A. Agarwal, S. Negahban, M. Wainwright, Noisy matrix decomposition via convex relaxation: Optimal rates in high dimensions, *Ann. Stat.* 40 (2) (2012) 1171–1197.
- [3] Y. Chen, A. Jalali, S. Sanghavi, C. Caramanis, Low-rank matrix recovery from errors and erasures, *IEEE Trans. Inform. Theory* 59 (7) (2013) 4324–4337.
- [4] R. Otazo, E. Candes, D. Sodickson, Low-rank and sparse matrix decomposition for accelerated dynamic mri with separation of background and dynamic components, *Magn. Reson. Med.* in press.
- [5] J. Wright, A. Ganesh, S. Rao, Y. Peng, Y. Ma, Robust principal component analysis: exact recovery of corrupted low-rank matrices by convex optimization, in: *NIPS*, 2009, pp. 2080–2088.
- [6] A. Waters, A. Sankaranarayanan, R. Baraniuk, SpaRCS: Recovering low-rank and sparse matrices from compressive measurements, in: *NIPS*, 2011, pp. 1089–1097.
- [7] M. Tao, X. Yuan, Recovering low-rank and sparse components of matrices from incomplete and noisy observations, *SIAM J. Optim.* 21 (1) (2011) 57–81.
- [8] Y. Liu, F. Shang, H. Cheng, J. Cheng, A Grassmannian manifold algorithm for nuclear norm regularized least squares problems, in: *UAI*, 2014.
- [9] E. Candes, X. Li, Y. Ma, J. Wright, Robust principal component analysis?, *J. ACM* 58 (3) (2011) 1–37.
- [10] T. Zhou, D. Tao, Greedy bilateral sketch, completion & smoothing, in: *AISTATS*, 2013, pp. 650–658.
- [11] Y. Zheng, G. Liu, S. Sugimoto, S. Yan, M. Okutomi, Practical low-rank matrix approximation under robust L1-norm, in: *CVPR*, 2012, pp. 1410–1417.
- [12] R. Cabral, F. Torre, J. Costeira, A. Bernardino, Unifying nuclear norm and bilinear factorization approaches for low-rank matrix decomposition, in: *ICCV*, 2013, pp. 2488–2495.
- [13] F. Shang, Y. Liu, J. Cheng, H. Cheng, Robust principal component analysis with missing data, in: *CIKM*, 2014.
- [14] R. Ma, N. Barzigar, A. Roozgard, S. Cheng, Decomposition approach for low-rank matrix completion and its applications, *IEEE Trans. Singal Proc.* 62 (7) (2014) 1671–1683.
- [15] Y. Peng, A. Ganesh, J. Wright, W. Xu, Y. Ma, RASL: Robust alignment by sparse and low-rank decomposition for linearly correlated images, *IEEE Trans. Pattern Anal. Mach. Intell.* 34 (11) (2012) 2233–2246.
- [16] Z. Li, J. Liu, Y. Jiang, J. Tang, H. Lu, Low rank metric learning for social image retrieval, in: *ACM Multimedia*, 2012, pp. 853–856.
- [17] Y. Liu, L. Jiao, F. Shang, F. Yin, F. Liu, An efficient matrix bi-factorization alternative optimization method for low-rank matrix recovery and completion, *Neur. Netw.* 48 (2013) 8–18.
- [18] Y. Feng, J. Xiao, Y. Zhuang, X. Yang, J. Zhang, R. Song, Exploiting temporal stability and low-rank structure for motion capture data refinement, *Inform. Sci.* (2014) in press.
- [19] G. Liu, Z. Lin, S. Yan, J. Sun, Y. Yu, Y. Ma, Robust recovery of subspace structures by low-rank representation, *IEEE Trans. Pattern Anal. Mach. Intell.* 35 (1) (2013) 171–184.
- [20] P. Favaro, R. Vidal, A. Ravichandran, A closed form solution to robust subspace estimation and clustering, in: *CVPR*, 2011, pp. 1801–1807.
- [21] H. Xu, C. Caramanis, S. Sanghavi, Robust PCA via outlier pursuit, in: *NIPS*, 2010, pp. 2496–2504.

- [22] X. Yuan, J. Yang, Sparse and low-rank matrix decomposition via alternating direction methods, *Pac. J. Optim.* 9 (1) (2013) 167–180.
- [23] E. Candes, B. Recht, Exact matrix completion via convex optimization, *Found. Comput. Math.* 9 (6) (2009) 717–772.
- [24] A. Eriksson, A. van den Hengel, Efficient computation of robust low-rank matrix approximations in the presence of missing data using the l_1 norm, in: *CVPR, 2010*, pp. 771–778.
- [25] J. Yu, Y. Rui, D. Tao, Click prediction for web image reranking using multimodal sparse coding, *IEEE Trans. Image Process.* 23 (5) (2014) 2019–2032.
- [26] M. Wang, B. Ni, X.-S. Hua, T.-S. Chua, Assistive tagging: A survey of multimedia tagging with human-computer joint exploration, *ACM Comput. Surv.* 44 (4).
- [27] D. Meng, Z. Xu, L. Zhang, J. Zhao, A cyclic weighted median method for L_1 low-rank matrix factorization with missing entries, in: *AAAI, 2013*.
- [28] K. Lee, J. Ho, D. Kriegman, Acquiring linear subspaces for face recognition under variable lighting, *IEEE Trans. Pattern Anal. Mach. Intell.* 27 (5) (2005) 684–698.
- [29] K. Min, Z. Zhang, J. Wright, Y. Ma, Decomposition background topics from keywords by principal component pursuit, in: *CIKM, 2010*, pp. 269–278.
- [30] X. Li, Compressed sensing and matrix completion with constant proportion of corruptions, *Constr. Approx.* 37 (2013) 73–99.
- [31] Z. Lin, R. Liu, Z. Su, Linearized alternating direction method with adaptive penalty for low-rank representation, in: *NIPS, 2011*, pp. 612–620.
- [32] S. Ma, D. Goldfarb, L. Chen, Fixed point and Bregman iterative methods for matrix rank minimization, *Math. Prog.* 128 (1) (2011) 321–353.
- [33] Y. Shen, Z. Wen, Y. Zhang, Augmented Lagrangian alternating direction method for matrix separation based on low-rank factorization, *Optim. Method Softw.* 29 (2) (2014) 239–263.
- [34] H. Avron, S. Kale, S. Kasiviswanathan, V. Sindhvani, Efficient and practical stochastic subgradient descent for nuclear norm regularization, in: *ICML, 2012*.
- [35] S. Boyd, N. Parikh, E. Chu, B. Peleato, J. Eckstein, Distributed optimization and statistical learning via the alternating direction method of multipliers, *Found. Trends Mach. Learn.* 3 (1) (2011) 1–122.
- [36] Z. Wen, W. Yin, Y. Zhang, Solving a low-rank factorization model for matrix completion by a nonlinear successive over-relaxation algorithm, *Math. Prog. Comp.* 4 (4) (2012) 333–361.
- [37] H. Nick, Matrix procrustes problems.
- [38] G. Liu, S. Yan, Active subspace: toward scalable low-rank learning, *Neur. Comp.* 24 (12) (2012) 3371–3394.
- [39] J. Cai, E. Candes, Z. Shen, A singular value thresholding algorithm for matrix completion, *SIAM J. Optim.* 20 (4) (2010) 1956–1982.
- [40] F. Shang, Y. Liu, J. Cheng, Generalized higher-order tensor decomposition via parallel ADMM, in: *AAAI, 2014*, pp. 1279–1285.
- [41] J. Yang, X. Yuan, Linearized augmented Lagrangian and alternating direction methods for nuclear norm minimization, *Math. Comp.* 82 (2013) 301–329.
- [42] R. Keshavan, A. Montanari, S. Oh, Matrix completion from a few entries, *IEEE Trans. Inform. Theory* 56 (6) (2010) 2980–2998.
- [43] M. Wang, R. Hong, G. Li, Z.-J. Zha, S. Yan, T.-S. Chua, Event driven web video summarization by tag localization and key-shot identification, *IEEE Trans. Multimedia* 14 (4) (2012) 975–985.
- [44] J. He, L. Balzano, A. Szlam, Incremental gradient on the Grassmannian for online foreground and background separation in subsampled video, in: *CVPR, 2012*, pp. 1568–1575.
- [45] D.-R. Liu, C.-H. Lai, W.-J. Lee, A hybrid of sequential rules and collaborative filtering for product recommendation, *Inform. Sci.* 179 (20) (2009) 3505–3519.
- [46] S. Lee, Y. Cho, S. Kim, Collaborative filtering with ordinal scale-based implicit ratings for mobile music recommendations, *Inform. Sci.* 180 (11) (2010) 2142–2155.
- [47] K.-C. Toh, S. Yun, An accelerated proximal gradient algorithm for nuclear norm regularized least squares problems, *Pac. J. Optim.* 6 (2010) 615–640.
- [48] R. Mazumder, T. Hastie, R. Tibshirani, Spectral regularization algorithms for learning large incomplete matrices, *J. Mach. Learn. Res.* 11 (2010) 2287–2322.
- [49] T. Ngo, Y. Saad, Scaled gradients on Grassmann manifolds for matrix completion, in: *NIPS, 2012*, pp. 1421–1429.
- [50] N. Boumal, P.-A. Absil, RTRMC: A Riemannian trust-region method for low-rank matrix completion, in: *NIPS, 2011*, pp. 406–414.
- [51] F. Shang, L. Jiao, F. Wang, Semi-supervised learning with mixed knowledge information, in: *KDD, 2012*, pp. 732–740.
- [52] F. Shang, L. Jiao, F. Wang, Graph dual regularization non-negative matrix factorization for co-clustering, *Pattern Recogn.* 45 (6) (2012) 2237–2250.

- [53] Z. Li, J. Liu, X. Zhu, T. Liu, H. Lu, Image annotation using multi-correlation probabilistic matrix factorization, in: ACM Multimedia, 2010, pp. 1187–1190.
- [54] J. Yu, D. Tao, M. Wang, Adaptive hypergraph learning and its application in image classification, IEEE Trans. Image Process. 21 (7) (2012) 3262–3272.
- [55] R. Tomioka, T. Suzuki, Convex tensor decomposition via structured Schatten norm regularization, in: NIPS, 2013, pp. 1331–1339.